J|A|C|S COMMUNICATIONS

Published on Web 07/09/2009

Walking a Supramolecular Tightrope: A Self-Assembled Dodecamer from an 8-Aryl-2′-deoxyguanosine Derivative

María del C. Rivera-Sánchez, Ivonne Andújar-de-Sanctis, Marilyn García-Arriaga, Vladimir Gubala, Gerard Hobley, and José M. Rivera*

Department of Chemistry, University of Puerto Rico, Río Piedras Campus, Río Piedras, Puerto Rico 00931

Received May 18, 2009; E-mail: jmrivortz@mac.com

Guanosine quadruplexes (GQs) have emerged in recent years as key players in the development of promising functional nanostructures.[1] GQs are formed by the self-assembly of guanosine subunits into planar tetramers (G-tetrads) that stack on each other, assisted by the complexation of a metal cation such as K^+ or Na^+. Alternatively, GQs can also form via the folding of G-rich oligonucleotides (e.g., DNA, RNA) leading to monomeric, dimeric, and tetrameric structures via the association of one, two, or four oligonucleotides, respectively.[1d,2] In the latter, the number of G-tetrads is primarily controlled by the sequence (intrinsic parameter) of the oligonucleotide, whereas, in the former, such control can be primarily achieved by adjusting extrinsic parameters (e.g., concentration, temperature, solvent,[3] the cation template,[4] and/or its counteranion[5]). Controlling the molecularity via intrinsic parameters (i.e., structural information in the supramolecular building blocks[6]) enables the reliable construction of nanostructures of well-defined size and composition. In recent years we have developed 8-aryl-2′-deoxyguanosine (8ArG) derivatives as versatile recognition motifs for the construction of supramolecular nanostructures in organic and aqueous media (Figure 1).[3a,7] For example, we have reported the reliable formation of a hexadecamer as the basis for constructing discrete self-assembled dendrimers.[7b] So far we have managed to adjust the intrinsic parameters of 8ArG's to program the preferential formation of octamers (O) or hexadecamers (H) (Figure 1b). However, using the same strategy to program the formation of the elusive intermediate dodecamer has proven more difficult.[7] Here we report on a lipophilic 8-(3-pyridyl)-2′-deoxyguanosine derivative that forms a discrete dodecamer with high fidelity[8] and enhanced stability relative to the octamer formed by an isosteric 8-phenyl-2′-deoxyguanosine derivative.

8ArG derivatives adopt a *syn* conformation around the glycosidic bond.[9] This limits the number of ways in which the resulting G-tetrads can orient themselves within the GQ (i.e., higher preorganization[10]). In most cases, the steric repulsion imposed by the groups attached to the ribose moiety in 8ArG's prevent the assembly beyond an octamer. However, this steric repulsion can be compensated by increasing the number of attractive noncovalent interactions. We have shown that carbonyl groups in the *meta* position of a phenyl moiety can engage in additional hydrogen bonds, among other noncovalent interactions, which enable the formation of a hexadecamer.[7] We hypothesized that derivatives with heteroaryl groups attached to C8 could engage in additional dipole−dipole interactions.[11] We expected these interactions to be strong enough to overcome the steric repulsion, enabling the formation of a dodecamer, but not too strong to drive the formation of a hexadecamer (Figure 1b).

To test this hypothesis, we studied the self-assembly in acetonitrile of 8-(3-pyridyl)-2′-deoxyguanosine esterified at the 3′ and 5′ positions with isobutyryl groups (**3PyGi**) and compared its behavior to that of the isosteric phenyl derivative (**PhGi**) (Figure 1a). Both compounds were prepared as previously described by us, using a Suzuki−Miyaura cross coupling reaction as the key synthetic step.[7d,12,13]

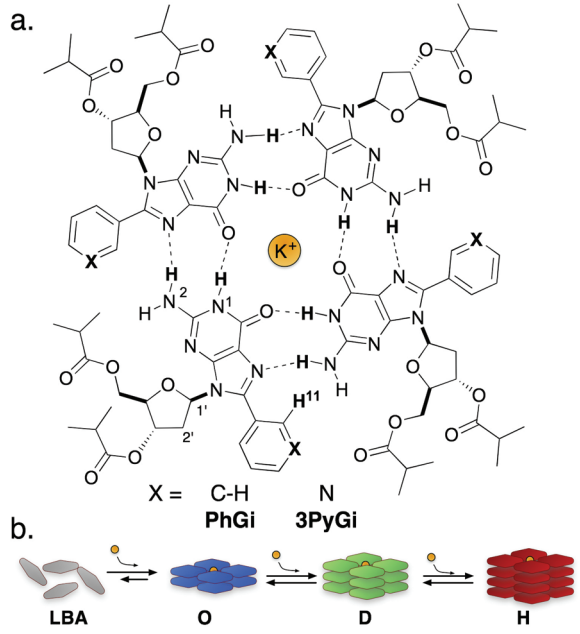

Figure 1. (a) Structure of the tetrad formed by **3PyGi** and **PhGi**. (b) Schematic representation of the various assemblies formed by 8ArG derivatives; LBA (Loosely Bound Aggregates), O (Octamer), D (Dodecamer), H (Hexadecamer).

^{1}H NMR titration studies of **PhGi** and **3PyGi** in CD_3CN, using K^+ as the templating cation, support the formation of an octamer and a dodecamer, respectively. Addition of increasing amounts of KI to a solution of **PhGi** reveals the disappearance of the peaks corresponding to loosely bound aggregates (LBA, Figures 1b, S6)[13] with the concomitant appearance of a new set of peaks that are consistent with an octamer of D_4 symmetry (O_{D4}) (Figure 2a). The corresponding experiments with **3PyGi** show a similar trend to **PhGi** with up to 0.06 equiv of KI added (Figure S7), suggesting the formation of a D_4-octamer.[13] Beyond this point, a new species with three sets of signals emerges (Figure S7),[13] becoming the main species (62% D, 34% O_{D4}) after the addition of 0.13 equiv of KI (Figure 2b). The spectral characteristics are consistent with the formation of a dodecamer of C_4 symmetry, where the highest fidelity[8] (94% D, 4% O_{D4}) was reached at 45 mM and 0.7 equiv of KI.[13] The speciation curves shown in Figure 3 summarize the results from these titration experiments.

Further support for the molecularities of $(\mathbf{3PyGi})_{12}$ and $(\mathbf{PhGi})_8$ comes from Vapor Pressure Osmometry (VPO) and 2D-DOSY experiments. VPO measurements provide a molecular weight for

a solution containing $(\mathbf{3PyGi})_{12}\cdot 2KI$ of 6216 Da with a calculated value of 5949 Da (Table S1).[13] A discrepancy of 267 Da, which is within the molecular weight of one subunit of **3PyGi** (485 Da), is very reasonable for this technique. Similar measurements with **PhGi** are also consistent with the formation of an octamer (4229 Da, Table S1).[13] DOSY experiments[14] provided diffusion coefficients (D, m^2s^{-1}) of $(5.69 \pm 0.05) \times 10^{-10}$, $(5.5 \pm 0.2) \times 10^{-10}$, and $(6.7 \pm 0.3) \times 10^{-10}$ for $(\mathbf{PhGi})_8$, $(\mathbf{3PyGi})_{12}$, and $(\mathbf{3PyGi})_8$, respectively.[13] Assuming a spherical shape, the Stokes−Einstein equation enables the following hydrodynamic radii (r, Å): 11.3 ± 0.1, 11.6 ± 0.2, and 9.5 ± 0.5, for $(\mathbf{PhGi})_8$, $(\mathbf{3PyGi})_{12}$, and $(\mathbf{3PyGi})_8$, respectively (Table S2).[13,14] The apparent discrepancy in the sizes for $(\mathbf{PhGi})_8$ and $(\mathbf{3PyGi})_8$ may result from a smaller amplitude in the "breathing" motions for the latter, due to its enhanced noncovalent interactions.

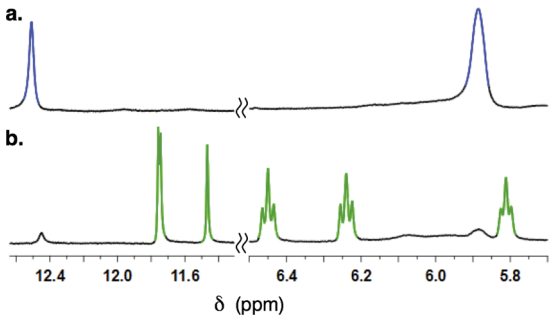

Figure 2. Partial ^{1}H NMR spectra (500 MHz, 298.2 K) of (a) **PhGi** and (b) **3PyGi** in CD_3CN with 0.7 equiv of KI. The peaks on the left (11.4−12.6 ppm) correspond to the N1H's, and those on the right (5.7−6.5 ppm) correspond to the CH1's.

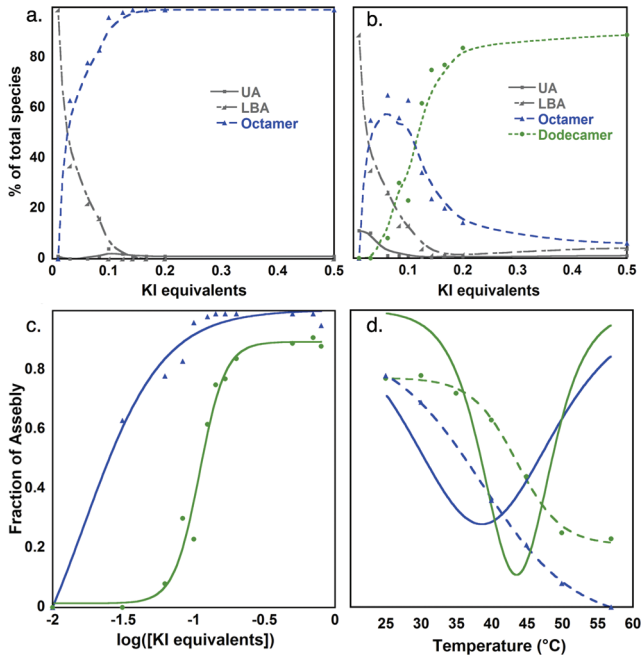

Figure 3. Speciation curves for (a) **PhGi** and (b) **3PyGi**. (c) Dose−response curves for $(\mathbf{PhGi})_8$ (blue) and $(\mathbf{3PyGi})_{12}$ (green) at 30 mM in CD_3CN at 298.2 K (Table S4).[13] (d) Melting profiles as determined by VT-NMR for $(\mathbf{PhGi})_8$ and $(\mathbf{3PyGi})_{12}$ (dashed blue and green lines, respectively) and the corresponding first derivative plots (solid lines). UA refers to unidentified assemblies.

The stability of both $(\mathbf{PhGi})_8$ and $(\mathbf{3PyGi})_{12}$ was assessed by variable concentration (VC) and variable temperature (VT) NMR experiments. VC studies in CD_3CN reveal that both $(\mathbf{PhGi})_8$ and $(\mathbf{3PyGi})_{12}$ compose greater than 90% of the mixtures above 20 mM and that significant amounts of assemblies are still detected upon dilution to 0.5 mM (Table S3, Figures S8−9).[13] However, diluting a solution of $(\mathbf{3PyGi})_{12}$ shifts the equilibrium toward $(\mathbf{3PyGi})_8$ until the ratio for both becomes 1:1 at 1 mM. The lower self-assembly concentration (lsac)[15] is 1−2 mM for both $(\mathbf{PhGi})_8$ and $(\mathbf{3PyGi})_{12}$. VT experiments reveal the enhanced thermodynamic stability of $(\mathbf{3PyGi})_{12}$ over $(\mathbf{PhGi})_8$, giving T_m values of 43.6 and 38.6 °C, respectively (Figures 3d, S10−11).[13] The higher stability of $(\mathbf{3PyGi})_{12}$ relative to $(\mathbf{PhGi})_8$ is likely due to the enhanced noncovalent interactions as discussed below.

Analysis of the titration data using a dose−response curve supports the notion that the assembly of both $(\mathbf{PhGi})_8$ and $(\mathbf{3PyGi})_{12}$ are cooperative processes. The calculated Hill coefficients (n_H) are 1.6 ± 0.5 and 4.8 ± 0.9, respectively (Figure 3c, Table S4).[13] The comparison and interpretation of such coefficients must be done with care, since the mechanism of formation of the octamer is likely to be different than that of the dodecamer.[16] Nonetheless, it is reasonable to state that the extent of cooperativity in the formation of $(\mathbf{3PyGi})_{12}$ is higher than that of $(\mathbf{PhGi})_8$.[17]

Computer modeling, supported by 2D NMR experiments, provides a compelling representation for the structure of $(\mathbf{3PyGi})_{12}$ and hints to the rationale for its formation. The information in the guanine moiety dictates how four 8ArG subunits organize themselves in a planar tetrad. Considering that the 8-aryl group preorganizes the subunits into the *syn* conformation, only one type of tetrad is possible. Since both octamers formed by **PhGi** and **3PyGi** are D_4-symmetric (as shown by NMR[13]), the interphases between the two tetrads must be homogeneous (i.e., head-to-head, *hh*, or tail-to-tail, *tt*; Figure 4b).[18] Intertetrad H2′(T1)−H2′(T2) NOE correlations support an *hh* interphase between those tetrads (Figures 4b, S18).[13] With this arrangement, the octamers formed by 8ArG's are stabilized by eight CH−π contacts between the C2′H_2 and the aryl rings in both T1 and T2 (Figure 4c). This is one of the reasons why quadruplexes made by 8ArG's are more stable, and self-assemble with greater fidelity, than those formed by the parent G.[7d] The formation of $(\mathbf{3PyGi})_{12}$ requires four additional subunits to assemble onto the existing $(\mathbf{3PyGi})_8$. The newly added tetrad (T3) orients itself with its "head" facing the "tail" of T2. This arrangement is supported by multiple NOEs including H1′(T2)−H1′(T3) and H11(T2)−H1′(T3) (Figure 4b), which would not be present with a *tt* interphase.[13]

In essence, the formation of $(\mathbf{3PyGi})_{12}$ is enabled by an optimum balance between repulsive and attractive noncovalent interactions, specifically, (i) cation−dipole interactions (somewhat offset by the electrostatic repulsion between the two templating cations); (ii) $\pi-\pi$ interactions, between T2 and T3; and (iii) dipole−dipole interactions between the pyridyl moieties (Figure 4d). Besides the dipole created by the nitrogen in the pyridyl ring, electron density surface maps (Figure 4e,f) show that opposite sides of such rings have slightly different electron densities that reinforce $\pi-\pi$ interactions. The formation of the dodecamer $(\mathbf{PhGi})_{12}$ is energetically unfavorable because the enhanced steric repulsion between the ester groups cannot be compensated by attractive dipole−dipole interactions like in $(\mathbf{3PyGi})_{12}$. Likewise, formation of the hexadecamer $(\mathbf{3PyGi})_{16}$ is prevented by a similar steric repulsion between the ester groups. At this stage, additional dipole−dipole interactions are not enough to stabilize such a hexadecamer.[3,7]

Guanine is an excellent information-rich recognition motif,[1] but there is significant ambiguity in that information,[6] leading to context dependent self-assembly.[3] This is not necessarily a disadvantage, and it is in fact often convenient for the elaboration of responsive systems. However, certain applications require a more reliable self-assembly, less ambiguity, which can only be achieved by modulat-

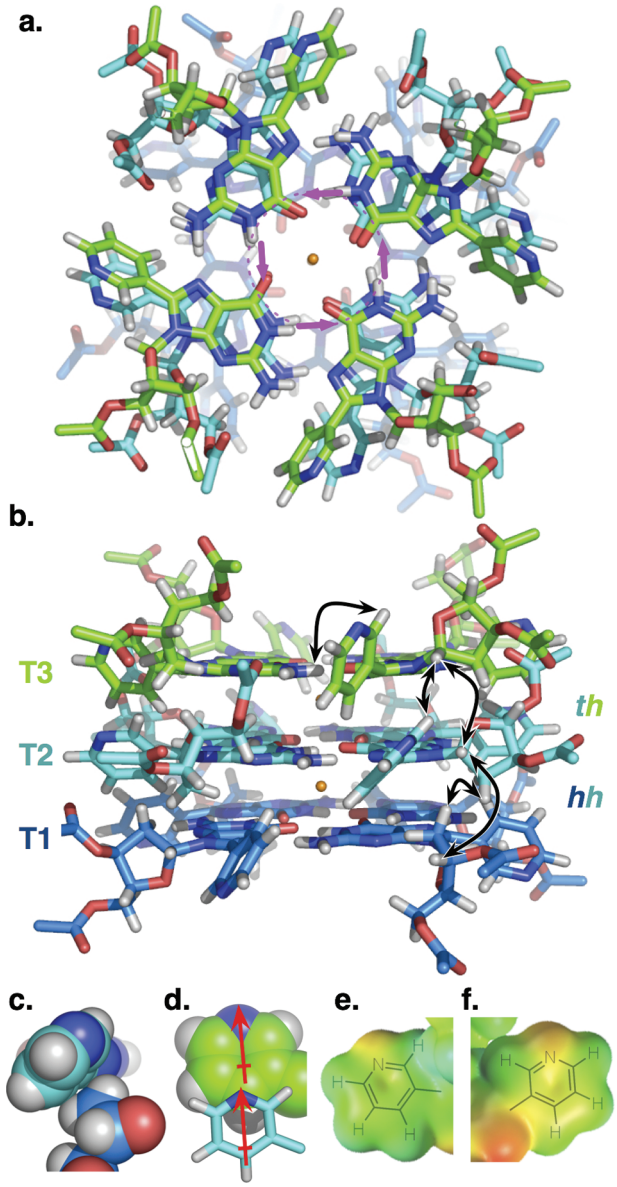

Figure 4. (a) Top and (b) side views for a model of (**3PyGi**)$_{12}$ where some atoms are omitted for clarity. (a) The top tetrad (T3) has its "tail" (i.e., rotation in the direction of the magenta arrows is counterclockwise, Figure S18)[13,18] facing up and its "head" in contact with the "tail" of the middle tetrad (T2). (b) T1 and T2 correspond to the initially formed octamer, and their interphase is *hh*. T3 assembles on T2 with an interphase of *th*. The black double-headed arrows show selected NOEs indicating intratetrad (T3) and intertetrad (T1−T2−T3) connectivities.[13] (c) Attractive CH−π interactions between the eight subunits in T1 and T2 stabilize (**PhGi**)$_8$ and (**3PyGi**)$_{12}$. (d) Dipole−dipole interactions between the subunits in T2 and T3 are only possible for **3PyGi** but not for **PhGi**. van der Waals surfaces with electrostatic potentials illustrate the difference in electron density between opposite sides of the pyridyl groups for subunits in (e) T3 and (f) T2, as viewed from the "head" and the "tail", respectively (see Figure S20 for more details).[13,19]

ing intrinsic parameters. The contrasting behavior of **PhGi** and **3PyGi** illustrates how specific information can be programmed[6] into 8ArG subunits by increasing their preorganization[10] and/or the number of contacts that engage in attractive interactions. This is why 8ArG derivatives are excellent platforms for the development of well-defined, predictable, and reliable supramolecular structures that form with high fidelity.[7]

We are currently studying the scope and limitations of other 8ArG derivatives that also show a propensity to form dodecamers. Adding these to the existing octamer- and hexadecamer-forming 8ArG derivatives will enable the preparation of a wide variety of self-assembled dendrimers and other nanostructures where the size and the number of functional elements can be fine-tuned for specific applications. The results of such studies will be reported in due course.

Acknowledgment. We thank NIH-SCoRE (2506GM08102) for financial support. M.C.R.S. thanks NASA-PR and PRIDCO, and M.G.A. thanks NIH-RISE for graduate fellowships. I.A.D. thanks the MARC program for an undergraduate fellowship.

Supporting Information Available: Detailed synthetic procedures, characterization for all new compounds, experimental protocols and NMR data. This material is available free of charge via the Internet at http://pubs.acs.org.

References

(1) (a) Davis, J. T.; Spada, G. P. *Chem. Soc. Rev.* **2007**, *36*, 296–313. (b) Alberti, P.; Bourdonclle, A.; Sacca, B.; Lacroix, L.; Mergny, J. L. *Org. Biomol. Chem.* **2006**, *4*, 3383–3391. (c) Spada, G. P.; Gottarelli, G. *Synlett* **2004**, 596–602. (d) Davis, J. T. *Angew. Chem., Int. Ed.* **2004**, *43*, 668–698.
(2) Neidle, S.; Balasubramanian, S. *Quadruplex Nucleic Acids*; The Royal Society of Chemistry Publishing: Cambridge, 2006.
(3) (a) Betancourt, J. E.; Martín-Hidalgo, M.; Gubala, V.; Rivera, J. M. *J. Am. Chem. Soc.* **2009**, *131*, 3186–3188. (b) González-Rodríguez, D.; Van Dongen, J.; Lutz, M.; Spek, A.; Schenning, A.; Meijer, E. *Nature Chem.* **2009**, *1*, 151–155.
(4) (a) Kwan, I. C.; She, Y.; Wu, G. *Chem. Commun.* **2007**, 4286–4288. (b) Cai, M. M.; Shi, X. D.; Sidorov, V.; Fabris, D.; Lam, Y. F.; Davis, J. T. *Tetrahedron* **2002**, *58*, 661–671.
(5) Shi, X. D.; Mullaugh, K. M.; Fettinger, J. C.; Jiang, Y.; Hofstadler, S. A.; Davis, J. T. *J. Am. Chem. Soc.* **2003**, *125*, 10830–10841.
(6) Lehn, J. M. *Science* **2002**, *295*, 2400–2403.
(7) (a) García-Arriaga, M.; Hobley, G.; Rivera, J. M. *J. Am. Chem. Soc.* **2008**, *130*, 10492–10493. (b) Betancourt, J. E.; Rivera, J. M. *Org. Lett.* **2008**, *10*, 2287–2290. (c) Gubala, V.; De Jesus, D.; Rivera, J. M. *Tetrahedron Lett.* **2006**, *47*, 1413–1416. (d) Gubala, V.; Betancourt, J. E.; Rivera, J. M. *Org. Lett.* **2004**, *6*, 4735–4738.
(8) Todd, E. M.; Quinn, J. R.; Park, T.; Zimmerman, S. C. *Isr. J. Chem.* **2005**, *45*, 381–389.
(9) Sessler, J. L.; Sathiosatham, M.; Doerr, K.; Lynch, V.; Abboud, K. A. *Angew. Chem., Int Ed.* **2000**, *39*, 1300–1303.
(10) Cram, D. *Angew. Chem., Int. Ed.* **1988**, *27*, 1009–1020.
(11) For a recent example on the use of dipole−dipole interactions to promote self-assembly, see: Li, Y.; Pink, M.; Karty, J. A.; Flood, A. H. *J. Am. Chem. Soc.* **2008**, *130*, 17293–17295.
(12) Hobley, G.; Gubala, V.; Rivera-Sánchez, M d. C.; Rivera, J. M. *Synlett* **2008**, 1510–1514.
(13) See Supporting Information.
(14) (a) Kaucher, M. S.; Lam, Y. F.; Pieraccini, S.; Gottarelli, G.; Davis, J. T. *Chem.—Eur. J.* **2005**, *11*, 164–173. (b) Cohen, Y.; Avram, L.; Frish, L. *Angew. Chem., Int. Ed.* **2005**, *44*, 520–554. (c) Macchioni, A.; Ciancaleoni, G.; Zuccaccia, C.; Zuccaccia, D. *Chem. Soc. Rev.* **2008**, *37*, 479–489.
(15) Lsac is the ratio at which assembled to disassembled species is 1:1. (a) Ercolani, G. *J. Phys. Chem. B* **1998**, *102*, 5699–5703. (b) Chi, X.; Guerin, A. J.; Haycoc, R. A.; Hunter, C. A.; Sarson, L. D. *J. Chem. Soc., Chem. Commun.* **1995**, 2563–2565.
(16) Ercolani, G. *J. Am. Chem. Soc.* **2003**, *125*, 16097–16103.
(17) Weiss, J. N *FASEB J.* **1997**, *11*, 835–841.
(18) The head of the tetrad is defined as the side in which rotation following the direction of the N1H's is clockwise. See Figure S18 for more information. Smith, F. W.; Lau, F. W.; Feigon, J. *Proc. Natl. Acad. Sci. U.S.A.* **1994**, *91*, 10546–10550.
(19) Molecular modeling was performed with *AMBER 94 (MacroModel)*, version 9.5, Maestro 8.0.315; Schrödinger, LLC: New York, 2007, using $CHCl_3$ as a continuum solvent. The electrostatic potential maps were calculated using the Hartree−Fock (3-21G) method from Spartan '08.

JA9040384